

Optimal mass and speed for interstellar flyby with directed-energy propulsion*

David G Messerschmitt^a, Philip Lubin^b, Ian Morrison^c

^a*University of California at Berkeley, Department of Electrical Engineering and Computer Sciences, USA*

^b*University of California at Santa Barbara, Department of Physics, USA*

^c*Curtin University, International Centre for Radio Astronomy Research, Australia*

Abstract

The design of mission scenarios for the flyby investigation of nearby star systems by probes launched using directed energy is addressed. Multiple probes are launched with a fixed launch infrastructure, and download of scientific data occurs following target encounter and data collection. Assuming the primary goal is to reliably recover a larger volume of collected scientific data with a smaller data latency (elapsed time from launch to complete recovery of the data), it is shown that there is an efficient frontier where volume cannot be increased for a given latency and latency cannot be reduced for a given volume. For each probe launch, increasing the volume along this frontier is achieved by increasing the probe mass, which results in a reduced probe speed. Thus choosing the highest feasible probe speed generally does not achieve an efficient tradeoff of volume and latency. Along this frontier the total distance traveled to the completion of data download does not vary significantly, implying that the download time duration is approximately a fixed fraction of the launch-to-target transit time. Due to longer propulsion duration when probe mass is increased, increasing data volume incurs a cost in the total launch energy expended, but with favorable economies of scale. An important characteristic of any probe technology is the scaling law that relates probe mass to transmit data rate, as this affects details of the efficient frontier.

Keywords: interstellar communications directed-energy flyby

*Copyright©2020

Preprint submitted to Elsevier

June 29, 2022

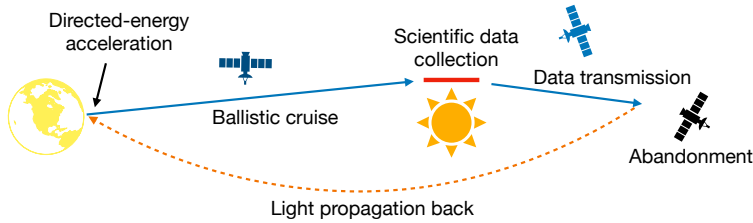


Figure 1: Illustration of the phases of a flyby mission for a probe propelled by directed energy from the launch site. The goal is to reliably recover the collected scientific data at the launch site.

1. Introduction

The advancement of propulsion technology for interstellar spacecraft and probes generally emphasizes achieving the maximum speed subject to cost constraints. In other words, subject to budget constraints, the greater the speed the better. This is a valid assumption in some cases, but not others. Here we address the specific case of a probe flyby mission for scientific data collection utilizing directed-energy propulsion, and show that manipulation of the probe speed is a beneficial design freedom to employ in addressing the needs of science investigators, who are the ultimate customers for the launch and data-return technology.

The development here is specific to directed energy, which does not provide deceleration. Thus it does *not* apply to missions entering an orbit or landing on a remote astronomical body, nor to propulsion technologies other than directed-energy. However, this special case illustrates how the ultimate purpose of a mission is an important consideration in the development of new propulsion technologies as well as in mission design. Parallel conclusions about matching spacecraft speed objectives to mission goals have been encountered in interstellar deceleration and landing missions [1, 2].

Directed-energy propulsion is attractive for flyby because it eliminates the need for a probe to carry fuel for propulsion, and this substantially reduces the mass at launch and thus enables a post-launch speed that is a significant fraction of light speed c . Such a flyby mission is assumed to consist of the phases illustrated in Fig.1. Since the directed-energy acceleration is short-lived relative to the total mission duration, it is reasonable to assume that the probe is ballistic; that is, it travels at a constant speed throughout the mission. The collection of a finite volume of scientific data (measured in bits) during target encounter is followed by downlink transmission following encounter, so the probe continues its ballistic trajectory for the duration of communication downlink operation.

The major cost of a flyby mission is a directed-energy beamer at the launch site, which may be terrestrial, on the moon, or a space platform. Assuming that

multiple probes are launched over time, the launch energy is a significant cost. Speeds in the range of $0.1c$ to $0.2c$ are often assumed¹ because they permit travel times to the nearest stars measured in decades, which is well within the duration of the typical career of a space scientist or engineer. An example of this is the ongoing StarShot project [3, 4, 5, 6]. To achieve these speeds with credible cost goals requires a small probe mass (perhaps 1 – 100 g). The major communication challenge is realizing a transmitter on the probe with a small mass budget and which can communicate back from interstellar distances.

2. Probe mass considerations in flyby missions

Because the directed-energy launcher is usually assumed to be shared over multiple launches, the launcher beam divergence and power are assumed to remain fixed, and the probe speed can be manipulated by changing the probe mass [7, 8, 5]. We show that performance metrics of direct interest to science investigators can be optimized by the choice of probe mass, since that mass indirectly affects the instrumentation carried by the probe and the data rate available during downlink operation, and because the probe speed affects the time available to perform science in the target vicinity and the time available to downlink data for a given termination distance.

For a flyby mission, the performance metrics of interest are listed in Tbl.1 and the design parameters available to manipulate those performance metrics are listed in Tbl.2. The primary purpose of a flyby mission is the collection of scientific data in the vicinity of the target followed by the reliable recovery of that data at or near the launch site. The performance metrics of primary interest to scientist investigators are the data volume $\mathcal{V}_{\text{data}}$ and the data latency T_{latency} . In other words, “how much data do we get back reliably, and how long do we have to wait for that data?” As will be seen, both these metrics are strongly influenced by the probe speed u_p . While domain scientists are usually not directly concerned with that speed, an exception is the impact on the time available for science investigations in the vicinity of the target. In this regard, slower (as advocated here) is always preferable.

2.1. Tradeoffs

Two mission design parameters are the duration of downlink transmission T_{down} , and the probe mass ratio ζ_p , which is proportional to the probe mass (where $\zeta_p = 1$ for some baseline case). If ζ_p is increased then it is appropriate to exploit that increased mass to increase the size of the probe’s sail, allowing the

¹At these speeds relativistic effects are not very significant (on the order of a few percent), so for the purposes of analyzing a flyby mission we employ classical approximations throughout.

Table 1: Flyby mission scientific performance metrics

Variable	Definition
$\mathcal{V}_{\text{data}}$	Total received volume of scientific data reliably recovered at Earth
T_{latency}	Data latency = time elapsed from launch to reception of scientific data in its entirety

Table 2: Flyby mission parameters

Variable	Definition
t	Classical coordinate time at launch site and at probe
T_{down}	Time duration of transmission in coordinate time
m_P	Mass of probe, including sail, instrumentation, and communications
ζ_P	Mass ratio, equal to m_P/m_0 , where m_0 is a baseline value for mass
u_P	Ballistic probe coordinate speed, with value u_0 for $\zeta_P = 1$
D_{star}	Distance from launch to target star, and from probe transmitter to receiver at the start of downlink operation
$\mathcal{R}_{\text{start}}$	Initial data rate at start of transmission, with value \mathcal{R}_0 for $\zeta_P = 1$
k	Mass ratio to data-rate scaling exponent, so the data rate \mathcal{R} scales by ζ_P^k

duration of acceleration to increase accordingly (see §4.1). Despite this longer acceleration, the probe speed decreases from a baseline value u_0 to $u_P < u_0$. The longer acceleration increases the energy expenditure, but that added energy expenditure is justified if the increased data volume is substantial (see §4.4).

Although the mission design parameters $\{\zeta_P, T_{\text{down}}\}$ can be varied to manipulate the mission performance metrics $\{\mathcal{V}_{\text{data}}, T_{\text{latency}}\}$, they should not be chosen arbitrarily. Rather, they should be jointly optimized to achieve the most favorable $\{\mathcal{V}_{\text{data}}, T_{\text{latency}}\}$ tradeoff. The impact of $\{\zeta_P, T_{\text{down}}\}$ on $\{\mathcal{V}_{\text{data}}, T_{\text{latency}}\}$ is slightly complicated, but can be summarized as:

- A larger ζ_P results in a smaller u_P .
- This increases the travel time to the target, and this increases T_{latency} .
- This results in a smaller accumulation of distance-squared propagation delay, and thus allows \mathcal{R} to decrease more slowly during downlink transmission, which in turn increases $\mathcal{V}_{\text{data}}$ (see §Appendix B).
- For fixed T_{down} , the probe has traveled less distance from the target during downlink operation, the maximum propagation delay back to the launch site is smaller, and this reduces T_{latency} .
- A larger probe mass budget for communications (including its electrical power generation) allows \mathcal{R} to be increased (see §Appendix B), and this increases $\mathcal{V}_{\text{data}}$.

While the travel-time increase is deleterious, all the other impacts are beneficial. Trading these off leads to an optimum point. We now summarize the conclusions of this optimization, followed by a supporting analysis in §4.

3. Optimal volume-latency tradeoff

The design of a data link, which conveys data reliably from probe to launch site, involves a number of interacting considerations such as wavelength, transmit aperture, receive collector, background radiation, modulation, and coding. For the purposes of mission design, all these considerations can be wrapped into a single parameter: a baseline data rate \mathcal{R}_0 at the beginning of downlink operation assuming $\zeta_p = 1$. The total data volume $\mathcal{V}_{\text{data}} \propto \mathcal{R}_0$, and thus it is convenient to use the normalized volume $\mathcal{V}_{\text{data}}/\mathcal{R}_0$ (which is dimensioned in time) as a performance metric to guide the choice of $\{\zeta_p, T_{\text{down}}\}$.

3.1. Efficient frontier

The tradeoff between $\mathcal{V}_{\text{data}}/\mathcal{R}_0$ and T_{latency} (first explored in [5]) is plotted in Fig.2. There exists a feasible region of operation $\{\mathcal{V}_{\text{data}}/\mathcal{R}_0, T_{\text{latency}}\}$, which is shaded in Fig.2. Points on the lower boundary of this region, called the *efficient frontier*², constitute all the advantageous mission operating points. That boundary yields the smallest possible T_{latency} for a given $\mathcal{V}_{\text{data}}/\mathcal{R}_0$, or the largest possible $\mathcal{V}_{\text{data}}/\mathcal{R}_0$ for a given T_{latency} .

Choice of a mission operation point somewhere on the efficient frontier provides flexibility in setting mission priorities. There are several compelling reasons to consciously select different operating points along the efficient frontier for different missions sharing a common launch infrastructure:

- Mission designers can consciously prioritize large $\mathcal{V}_{\text{data}}/\mathcal{R}_0$ or small T_{latency} .
- Different probes may carry different types of instrumentation, and these impose different mass and data volume requirements.
- There will likely be an evolution of probe technology over time. Early probes may emphasize technology validation with low T_{latency} (and hence small $\mathcal{V}_{\text{data}}/\mathcal{R}_0$), while later probes may emphasize scientific return with larger $\mathcal{V}_{\text{data}}/\mathcal{R}_0$ (and hence larger T_{latency}).
- There may be missions to different targets at different distances (within the solar system and interstellar), significantly changing the possible range of T_{latency} .

²This terminology is borrowed from a similar concept in financial portfolio theory [9]. It is a special case of the *Pareto frontier* (Pareto optimization is widely employed in various engineering disciplines [10]).

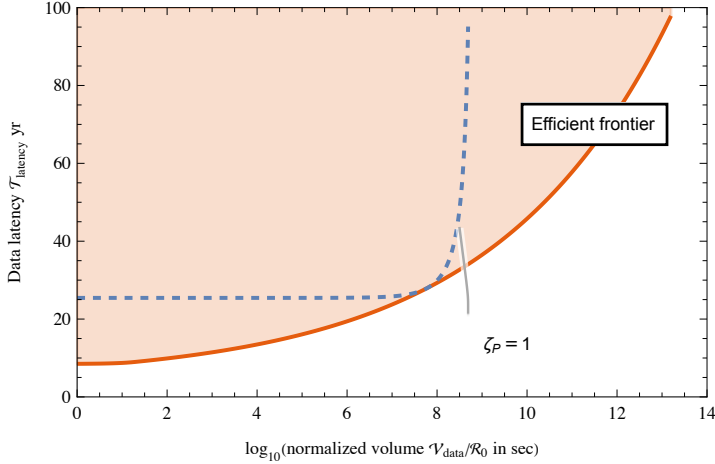


Figure 2: Plots of data latency T_{latency} (in years) vs the log of the normalized data volume $\mathcal{V}_{\text{data}}/\mathcal{R}_0$ (in seconds) where \mathcal{R}_0 is the data rate (in bits per second) at the beginning of downlink transmission (data rate declines from there as the square of propagation distance) for mass ratio $\zeta_p = 1$. $\mathcal{V}_{\text{data}}$ (in bits) is found by multiplying by the assumed value for \mathcal{R}_0 . Any volume-latency mission operating point within the shaded region is feasible. The lower boundary of this region, called the efficient frontier, is an efficient operating point in the sense of maximizing the volume for a given latency, or minimizing latency for a given volume. The set of operation points obtained by fixing $\zeta_p = 1$ and varying downlink operation duration T_{down} are shown as a dashed curve.

Generally mission designers will seek to maximize an objective function that combines volume and latency objectives. Only points along the efficient frontier need be considered in any such optimization.

Also illustrated in Fig.2 as the dashed curve is a set of possible mission operation points when a baseline value $\zeta_p = 1$ is chosen and only T_{down} is varied. This arbitrary choice of ζ_p permits operation at exactly one point on the efficient frontier through a judicious choice of T_{down} . More generally, achieving an arbitrary operating point on the efficient frontier requires a coordinated choice of $\{\zeta_p, T_{\text{down}}\}$ rather than constraining ζ_p in this manner.

3.2. Origin of efficient frontier

Additional insight into the efficient frontier follows from examining the fixed ζ_p dashed curve. Its general shape follows from two asymptotes as illustrated in Fig.3a. For small $\mathcal{V}_{\text{data}}/\mathcal{R}_0$ the horizontal asymptote is due to the minimum possible data latency T_{latency} when $T_{\text{down}} \rightarrow 0$. In this event downlink operation duration is not a factor and T_{latency} becomes dominated by the sum of launch-to-target transit time and signal propagation time back to the receiver. Similarly, $\mathcal{V}_{\text{data}}/\mathcal{R}_0$ is bounded from above by a vertical asymptote, which follows from the

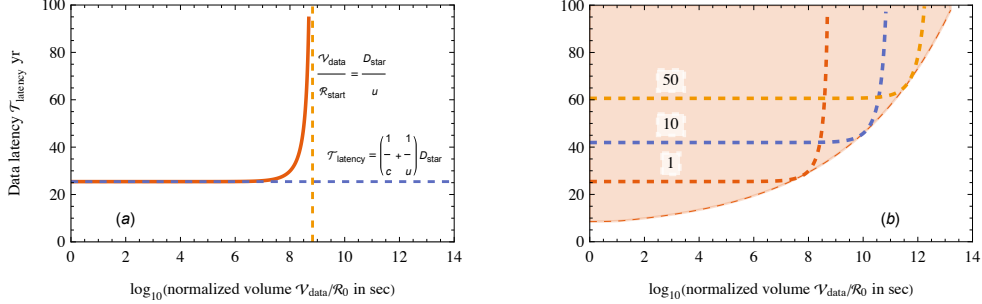


Figure 3: An illustration of the fixed mass ratio ζ_P operating points as the downlink operation duration T_{down} is varied. (a) The dashed curve in Fig.2 is interpreted in terms of its two asymptotes, one determined by the minimum possible T_{latency} and the other determined by the maximum possible $\mathcal{V}_{\text{data}}/\mathcal{R}_0$. (b) A repeat of Fig.2 showing $\zeta_P \in \{1, 10, 50\}$. Increasing ζ_P results in an increase in the minimum latency asymptote (due to a reduction in the probe speed) as well as an increase in the $\mathcal{V}_{\text{data}}/\mathcal{R}_0$ asymptote (due to a slower reduction in \mathcal{R}).

maximum $\mathcal{V}_{\text{data}}$ as $T_{\text{down}} \rightarrow \infty$. The increasing distance of the probe during downlink operation reduces the data rate \mathcal{R} as distance-squared, and the integral of \mathcal{R} is finite even as T_{down} becomes arbitrarily large. The efficient frontier is achieved by a judicious choice of an appropriate T_{down} intermediate to these two asymptotes. Varying the fixed value of ζ_P results in a family of curves as illustrated in Fig.3b. The efficient frontier is the lower envelope of this family of curves.

3.3. Data rate scaling law

The details of the efficient frontier are affected by the relationship between ζ_P and \mathcal{R} . Actually \mathcal{R} is directly related to a second mass ratio ζ_C , which is the factor by which the mass of the communications subsystem is increased even as the mass of the entire probe is increased by ζ_P . It is shown in §4.2 that under two distinct but reasonable sets of assumptions $\zeta_C \geq \zeta_P$, so the mass-ratio budget available for communications is at least as generous as for the probe in its entirety. When a communications subsystem is much lighter than the remainder of the payload, and a disproportionate part of any mass increase is devoted to communications, ζ_C can potentially be much larger than ζ_P .

\mathcal{R} is proportional to the product of transmit power and the transmit aperture area, among other factors (such as receive collector area). In view of this, there are two distinct ways in which $\zeta_C > 1$ can be exploited to increase \mathcal{R} :

Increased electrical power: Electrical power can be increased by ζ_C . As an existence proof, for any given electrical generator technology the replication of J such generators results in a mass and power that is a factor of J larger.

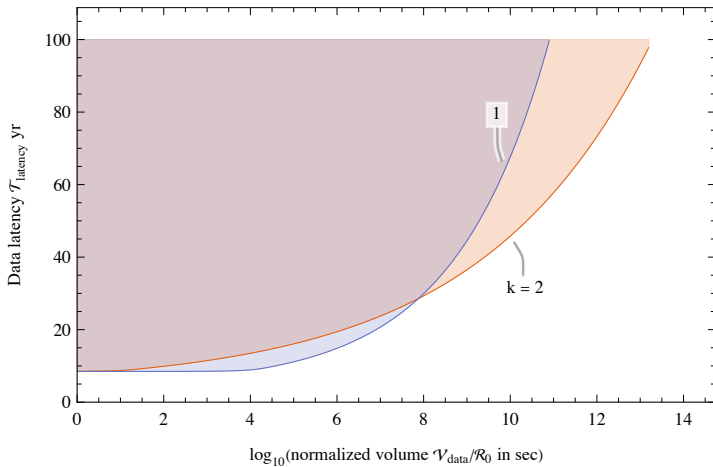


Figure 4: The efficient frontier in Fig.2 is compared for scaling exponents $k = 2$ and $k = 1$. The proportional case ($\zeta_C = \zeta_P$) is assumed.

Consolidating these generators into fewer and larger is worthwhile only if the outcome is a materially improved power-to-mass ratio.

Increased transmit aperture area: If the radiation area of a transmit aperture is increased by a factor of J , then its mass may need to be no more than J times larger. However, the available aperture fabrication technology may not offer quite this favorable a tradeoff, if for example additional mass may be necessary as a means to strengthen the larger structure. There also may be other limitations on transmit aperture area, such as the available pointing accuracy. The transmit aperture area should be matched to that pointing accuracy, so that the beam divergence is sufficiently large (aperture area sufficiently small) to cover the receiver in the presence of the worst-case pointing offset.

These observations suggest that the data rate $\mathcal{R}_{\text{start}}$ at the start of downlink operation can be related to ζ_C through

$$\mathcal{R}_{\text{start}} = \zeta_C^k \mathcal{R}_0 \quad (1)$$

and $1 \leq k \leq 2$ is a transmit power *scaling exponent*. The $k = 1$ case would apply when the transmit aperture size is not increased at all, and $k = 2$ would apply if the benefits of increased mass on both power and area are fully exploited. The efficient frontier for these extreme cases is compared in Fig.4. Not surprisingly $k = 2$ is preferred because it can achieve one to two orders of magnitude larger $\mathcal{V}_{\text{data}}/\mathcal{R}_0$.

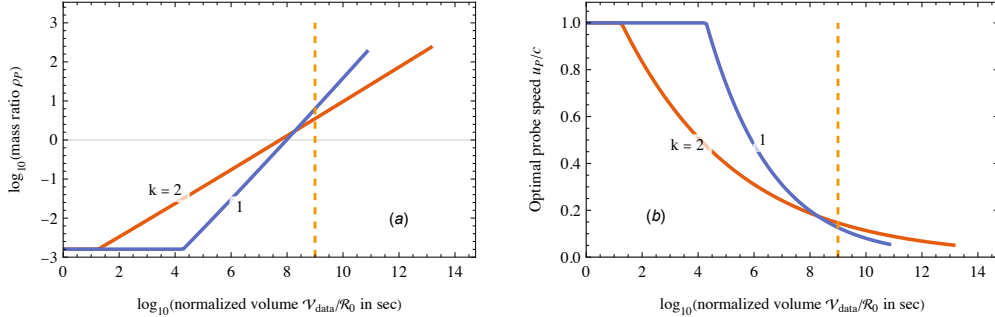


Figure 5: Assuming operation on the efficient frontier in Fig.4, a log plot of the optimal mass ratio ζ_P in (a) and a plot of the resulting probe speed as a fraction of the light speed in (b) assuming baseline speed $u_0 = 0.2c$ at $\zeta_P = 1$. The two scaling exponents $k \in \{1, 2\}$ are plotted and labeled. The vertical dashed line illustrates one data volume of interest, which is $\mathcal{V}_{\text{data}} = 10^9$ bits (1 Gb) at a baseline data rate $\mathcal{R}_0 = 1$ bits s^{-1} at the beginning of downlink operation. $\zeta_P \ll 1$ achieves low data latency by increasing the probe speed and thus reducing the transit time to the target (at the expense of a low data volume). $\zeta_P \gg 1$ achieves a larger data volume by reducing the probe speed (resulting in a larger data latency).

3.4. Other dependent mission parameters

The mass ratio ζ_P (in conjunction with k) is the independent mission parameter that affects the operating point along the efficient frontier. Since a specific point on the efficient frontier corresponds to a specific choice of $\{\zeta_P, T_{\text{down}}\}$, other mission parameters that must be chosen are dependent on this.

The value of ζ_P is shown in Fig.5a for the assumptions underlying Fig.4. This has the secondary effect of determining the probe speed u_P as shown in Fig.5b. With increasing $\mathcal{V}_{\text{data}}/\mathcal{R}_0$, the mass ratio increases and the speed decreases. Increasing $\mathcal{V}_{\text{data}}/\mathcal{R}_0$ and operating on the efficient frontier also requires an increase in transmission time T_{down} , as shown in Fig.6a. However, the transit time from launch to target also increases due to lower probe speed, and the ratio of T_{down} to that transit time remains relatively constant as shown in Fig.6b. Since both transit time and downlink operation duration scale with probe speed, the actual distance traveled by the probe during downlink operation doesn't vary much at different points on the efficient frontier.

The overall conclusion is that the squared-distance dependency of \mathcal{R} is the dominant consideration. That results in a distance traveled from launch to the end of downlink transmission that is relatively invariant across different operating points on the efficient frontier. The primary tool for adjusting the volume-latency tradeoff on the frontier is probe speed rather than distance traveled during downlink transmission.

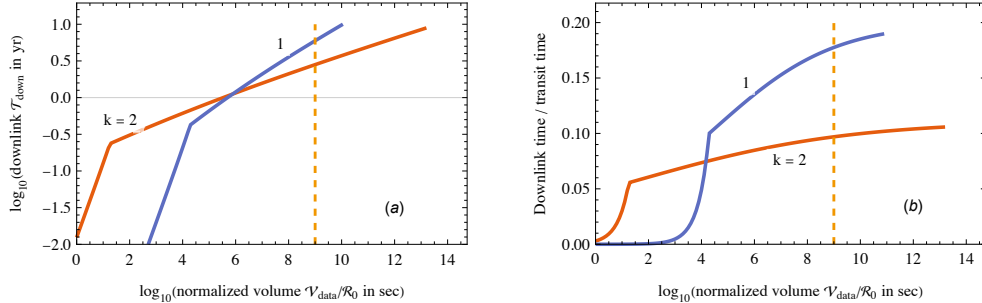


Figure 6: Under the same conditions as Fig.5, a plot of (a) the log of the optimal downlink operation duration T_{down} and (b) the ratio of T_{down} to the transit time from launch to target. A rule of thumb is that for $\zeta_P \gg 1$, this ratio should be about 9% for $k = 2$ and 17% for $k = 1$. The distance flown during downlink operation has the same relationship to the launch-to-target distance.

4. Analysis

An analytic treatment of the volume-latency tradeoff provides additional insight.

4.1. Directed energy kinematics

The total probe mass m_P can be broken into constituents as

$$m_P = m_C + m_E + m_S, \quad (2)$$

where m_C is the communications subsystem, m_S is the sail, and m_E is everything else (including attitude control, pointing, and scientific instrumentation). Electric power generation serves communication, scientific instrumentation and attitude control, but communication and instrumentation can share generation capacity since they do not need to operate concurrently.

The kinematics of a directed-energy launch was studied in [7] and is reviewed in §Appendix A. This establishes that the m_S should always make up exactly half of m_P in order to achieve the maximum probe speed during the ballistic phase of the mission. With this optimum m_S , the probe speed scales as $u_P \propto \zeta_P^{-1/4}$. The total launch energy scales as $\mathcal{E}_{\text{launch}} \propto \zeta_P^{3/4}$. Thus the launch energy increases as the probe speed decreases because the directed-energy beam takes longer to reach the diffraction limit with a larger sail.

Example: When $\zeta_P = 16$, the probe speed u_P is reduced by a factor of $16^{1/4} = 2$ and the launch energy $\mathcal{E}_{\text{launch}}$ is increased by a factor of $16^{3/4} = 8$. For scaling exponent $k = 2$ the data rate $\mathcal{R}_{\text{start}}$ immediately following encounter is increased by a factor of $16^2 = 256$, which increases the normalized data volume $\mathcal{V}_{\text{data}}/\mathcal{R}_0$ by that same factor.

4.2. Mass allocation

Communication mass ratio ζ_C may beneficially be larger than ζ_P , as now discussed. Assume the baseline probe masses $\{m_{P,0}, m_{C,0}, m_{E,0}, m_{S,0}\}$ associated with the mass categories in Eq.(2), and the variation of mass across different probe missions can be expressed in the mass ratios

$$\zeta_P = \frac{m_P}{m_{P,0}}, \text{ and } \zeta_C = \frac{m_C}{m_{C,0}}. \quad (3)$$

The kinetic law $m_P = 2m_S$ is also assumed, with the result that ζ_P determines the probe speed u_0 as described in §4.1. The other mass ratio ζ_C determines how much resource can be devoted to achieving an initial data rate $\mathcal{R}_{\text{start}}$. Thus the relationship between ζ_P and ζ_C is significant. We address this question under two alternative assumptions:

Proportional masses: As m_P is varied, $m_C \propto m_E$, in which case $\zeta_C = \zeta_P$. Thus an increase in m_P provides an equivalent benefit (in terms of mass ratio) to the communications and instrumentation subsystems. Not only can $\mathcal{R}_{\text{start}}$ be increased, but also the mass devoted to instrumentation can be increased. These two increases may go hand in hand, if for example a more massive instrumentation benefits from a larger data volume.

Fixed mass: As m_P is varied m_E is kept fixed, so the entirety of a probe mass m_P increase is devoted to increasing m_C . In this case the fraction of the mass devoted to communications becomes relevant. An additional mass ratio is defined,

$$\gamma = \frac{m_{C,0}}{m_{C,0} + m_E}. \quad (4)$$

Overall we find that

$$\zeta_C = \begin{cases} \zeta_P, & \text{proportional} \\ 1 + \frac{\zeta_P - 1}{\gamma}, & \text{fixed} \end{cases}. \quad (5)$$

Since $0 < \gamma < 1$ it follows that $\zeta_P \leq \zeta_C$, with equality at the limit as $\gamma \rightarrow 1$. For low-mass probes we would expect a γ to be relatively large, say $\gamma \approx 0.5$, which results in smaller impact on ζ_C than for a massive spacecraft. The fixed case is always more favorable to communications since the entirety of any mass increase benefits the communications subsystem. To the extent that ζ_C is larger than ζ_P , this benefits $\mathcal{V}_{\text{data}}/\mathcal{R}_0$ as illustrated in Fig.7.

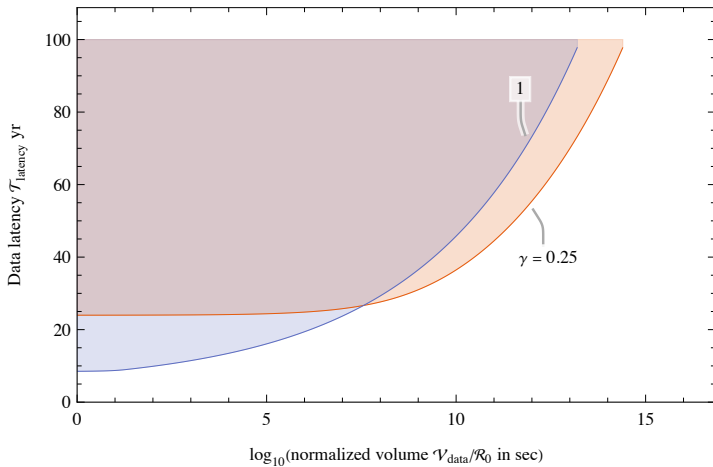


Figure 7: Repeating Fig.4, and the scaling exponent $k = 2$, the efficient frontier is plotted for two values $\gamma \in \{1, 0.25\}$. The $\gamma = 1$ case assumes that the mass change devoted to communications is proportional to the total mass change. The $\gamma = 0.25$ case assumes that the total non-communication mass (exclusive of sail) is $3\times$ larger than the communications subsystem mass at the baseline, and further that non-communication mass remains fixed as any mass change along the efficient frontier is allocated entirely to communications. This $\gamma = 0.25$ case magnifies the impact of that mass change on $\mathcal{V}_{\text{data}}/\mathcal{R}_0$ because of the disproportionate effect on $\mathcal{R}_{\text{start}}$.

4.3. Determination of efficient frontier

The efficient frontier is found by numerical minimization of T_{latency} with respect to ζ_P for each value of $\mathcal{V}_{\text{data}}/\mathcal{R}_0$ of interest (see §Appendix B). An approximation that avoids the numerical minimization follows by assuming (based on the numerical results of Fig.6b) that the downlink operation time T_{down} is a constant fraction of the launch-to-encounter time (see §Appendix C).

4.4. Launch energy cost and economies of scale

Although the launch infrastructure remains fixed, the variable launch costs increase as $\mathcal{V}_{\text{data}}/\mathcal{R}_0$ increases along the efficient frontier. This is because an increase in ζ_P implies an increase in launch energy in spite of the lower probe speed (see §Appendix A). Launch energy $\mathcal{E}_{\text{launch}}$ is plotted in Fig.8a.

Also shown in Fig.8b is the ratio of $\mathcal{E}_{\text{launch}}$ to $\mathcal{V}_{\text{data}}/\mathcal{R}_0$, which decreases steadily. If we view $\mathcal{E}_{\text{launch}}$ as a primary variable cost of scientific data return and a larger $\mathcal{V}_{\text{data}}/\mathcal{R}_0$ as the reward for that expenditure, then data return exhibits significant economies of scale. In particular, increasing ζ_P in the interest of a larger $\mathcal{V}_{\text{data}}$ incurs a lower cost than launching duplicative less massive probes to achieve the same overall $\mathcal{V}_{\text{data}}$. Of course other system objectives such as reliability and diversity of scientific instrumentation should be taken into account as well.

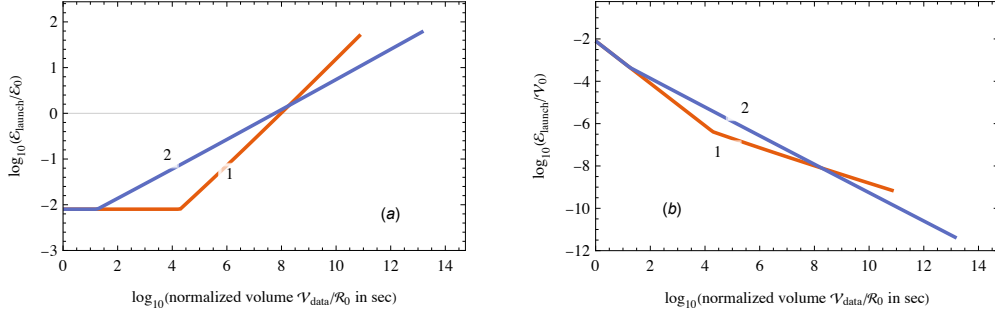


Figure 8: For operation on the efficient frontier in Fig.4, a log plot of the relationship of launch energy $\mathcal{E}_{\text{launch}}$ to normalized data volume $\mathcal{V}_{\text{data}}/\mathcal{R}_0$. The two scaling exponents $k \in \{1, 2\}$ are plotted and labeled. (a) $\mathcal{E}_{\text{launch}}$ increases with data volume because of the larger mass probe that is necessitated to achieve that volume. (b) The ratio of $\mathcal{E}_{\text{launch}}$ to $\mathcal{V}_{\text{data}}/\mathcal{R}_0$ decreases steadily, demonstrating that additional $\mathcal{V}_{\text{data}}/\mathcal{R}_0$ comes at a lower and lower incremental cost in terms of launch energy.

5. Conclusions

This study undermines any presumption for interstellar missions that the maximum probe speed should be achieved. To ascertain the best choice of speed, the needs of the ultimate stakeholders should be assessed, leading to optimized mission parameters. For the mission scenario considered here, with an emphasis on performance parameters ultimately of interest to domain science investigators in a directed-energy flyby mission, the conclusion is that any concrete choice of probe speed can achieve only a single point on the efficient frontier, and achieving other optimal volume-latency tradeoffs requires an appropriate choice of probe mass ratio and thus speed. Further, this optimization determines other mission parameters such as transmission time, and secondarily the launch energy requirement. The remaining degree of freedom is the data volume-latency tradeoff, which is achieved by moving along the efficient frontier. An additional consideration is the instrumentation (as to both mass and electrical power requirements) which may also influence the choice of probe mass as well.

While the efficient frontier is a universal concept, its particulars are dependent on the mass-to-data-rate scaling law, which is an important characteristic of any assumed probe technology and design, and is also affected by the choice of instrumentation. Also, the results and conclusions apply to directed-energy propulsion with a fixed launcher infrastructure, with the only launch parameter dependent on probe mass being the duration of launch acceleration. This is a natural assumption for a launcher that is shared among multiple probes with heterogenous instrumentation, data volume, and latency preferences.

6. Acknowledgements

The contribution of anonymous reviewers to improvement in this paper is appreciated.

PML funding for this program comes from NASA grants NIAC Phase I DEEP-IN ? 2015 NNX15AL91G and NASA NIAC Phase II DEIS 2016 NNX16AL32G and the NASA California Space Grant NASA NNX10AT93H and the Emmett and Gladys W. Technology Fund as well as from Limitless Space Institute and Breakthrough Initiatives.

Appendix A. Launcher-sail analysis

We employ a classical model, which gives results approximating a relativistic model [11] as long as the probe speed remains in the sub-relativistic regime ($u_p < 0.5c$ or so). At higher speeds a relativistic model is indicated.

Assume that the beamer directs a fixed power at the sail for a time period T_{launch} , and all that power is reflected by the sail (that is the sail remains within the diffraction limit throughout the acceleration). Then the force F and acceleration a on the sail both remain constant throughout acceleration. Assume the total mass of the probe is m_p , and this includes the sail mass m_s . The kinematics can then be summarized by

$$F = m_p a, \quad (aT_{\text{launch}}^2/2) \propto \sqrt{m_s}, \quad u_p = aT_{\text{launch}}.$$

The distance over which acceleration occurs (until the diffraction limit is reached) is proportional to the diameter of the sail, which in turn is proportional to $\sqrt{m_s}$, leading to the second equation. Solving for u_p and differentiating establishes that the maximum ballistic speed u_p is achieved for the choice $2m_s = m_p$. Adopting this value for m_s , the result is that $u_p \propto m_p^{-1/4}$. A further conclusion is that $T_{\text{launch}} \propto m_p^{3/4}$, and thus the launch energy $\mathcal{E}_{\text{launch}} \propto \zeta^{3/4}$.

Appendix B. Volume-latency relations

The achievable \mathcal{R} for any efficient communication link design is proportional to received power, which follows a distance-squared law. Thus for a given starting data rate $\mathcal{R}_{\text{start}}$, the best achievable data rate as a function of coordinate time t decreases as,

$$\frac{\mathcal{R}[t]}{\mathcal{R}_{\text{start}}} = \left(\frac{D_{\text{star}}}{D_{\text{star}} + u_p t} \right)^2.$$

The total data volume follows by integration,

$$\frac{\mathcal{V}_{\text{data}}}{\mathcal{R}_{\text{start}}} = \int_{t_1=0}^{T_{\text{down}}} \frac{\mathcal{R}[t]}{\mathcal{R}_{\text{start}}} \cdot dt = \frac{D_{\text{star}} T_{\text{down}}}{D_{\text{star}} + u_p T_{\text{down}}} \xrightarrow{T_{\text{down}} \rightarrow \infty} \frac{D_{\text{star}}}{u_p}. \quad (\text{B.1})$$

There are two profound implications. First, $\mathcal{V}_{\text{data}}$ in Eq.(B.1) increases as u_P decreases because of the slower rate of increase in propagation loss. Second, $\mathcal{V}_{\text{data}}$ is bounded even when the energy available for transmission is unlimited.

The data latency is given by

$$T_{\text{latency}} = (D_{\text{star}} + u_P T_{\text{down}}) \left(\frac{1}{u_P} + \frac{1}{c} \right). \quad (\text{B.2})$$

where the first term is the total distance flown to the end of downlink operation and the second term takes into account both the transit time to that distance and the signal propagation time back from that distance.

Eq.(B.1) and Eq.(B.2) can then be solved simultaneously to obtain $\{T_{\text{latency}}, T_{\text{down}}\}$ as a function of $\mathcal{V}_{\text{data}}/\mathcal{R}_0$,

$$T_{\text{latency}} = \frac{D_{\text{star}}^2 \mathcal{R}_{\text{start}}}{D_{\text{star}} \mathcal{R}_{\text{start}} - u_P \mathcal{V}_{\text{data}}} \left(\frac{1}{u_P} + \frac{1}{c} \right), \quad T_{\text{down}} = \frac{D_{\text{star}} \mathcal{V}_{\text{data}}}{D_{\text{star}} \mathcal{R}_{\text{start}} - u_P \mathcal{V}_{\text{data}}}. \quad (\text{B.3})$$

The domain of applicability was determined in Eq.(B.1). The scaling laws in Eq.(1), Eq.(5), and from §4.1 can be substituted. The efficient frontier is then obtained by numerically minimizing T_{latency} with respect to ζ_P for each value of $\mathcal{V}_{\text{data}}/\mathcal{R}_0$ of interest. The compatible value for T_{down} then follows directly from Eq.(B.3).

Appendix C. Approximation to efficient frontier

Examining Fig.6b, the numerical minimization in determining the efficient frontier can be avoided by choosing an approximate downlink operation time

$$T_{\text{down}} \simeq b \cdot D_{\text{star}}/u_P, \quad (\text{C.1})$$

where $b \approx 0.09$ for $k = 2$ and $b \approx 0.17$ for $k = 1$. The resulting efficient frontier (as a curve parameterized by ζ_P) is

$$\mathcal{V}_{\text{data}}/\mathcal{R}_0 \approx \frac{b D_{\text{star}} \zeta_P^{1/4} \left(\frac{\gamma + \zeta_P - 1}{\gamma} \right)^k}{(b+1) u_0}, \quad T_{\text{latency}} \approx (b+1) D_{\text{star}} \left(\frac{1}{c} + \frac{\zeta_P^{1/4}}{u_0} \right). \quad (\text{C.2})$$

The accuracy of this approximation can be verified by numerical comparison.

References

- [1] A. Bond, A. R. Martin, Project daedalus reviewed, Journal of the British interplanetary society 39 (9) (1986) 385–390.

- [2] K. Long, R. Obousy, A. Tziolas, A. Mann, R. Osborne, A. Presby, M. Fogg, Project icarus: Son of daedalus, flying closer to another star, arXiv preprint arXiv:1005.3833 (2010).
- [3] K. L. Parkin, The breakthrough starshot system model, *Acta astronautica* 152 (2018) 370–384.
- [4] K. Parkin, A starshot communication downlink, arXiv preprint arXiv:2005.08940 (October 2019).
- [5] D. G. Messerschmitt, P. Lubin, I. Morrison, Challenges in scientific data communication from low-mass interstellar probes, *The Astrophysical Journal Supplement Series* 249 (2) (2020) 36.
- [6] D. Messerschmitt, P. Lubin, I. Morrison, Technological challenges in low-mass interstellar probe communication, in: *Tennessee Valley Interstellar Symposium*, Wichita, KN, 2019.
- [7] P. Lubin, A roadmap to interstellar flight, *Journal of the British Interplanetary Society* 69 (2016). arXiv:arXiv:1604.01356.
- [8] P. Lubin, W. Hettel, The path to interstellar flight, *Acta Futura* 12 (2020) 9–44. doi: 10.5281/zenodo.3874099.
URL <https://doi.org/10.5281/zenodo.3874099>
- [9] R. Merton, An analytic derivation of the efficient portfolio frontier, *Journal of financial and quantitative analysis* 7 (4) (1972) 1851–1872.
- [10] W. Jakob, C. Blume, Pareto optimization or cascaded weighted sum: A comparison of concepts, *Algorithms* 7 (1) (2014) 166–185.
- [11] N. Kulkarni, P. Lubin, Q. Zhang, Relativistic spacecraft propelled by directed energy, *The Astronomical Journal* 155 (4) (2018) 155. doi:10.3847/1538-3881/aaafd2.